THE BELL SYSTEM TECHNICAL JOURNAL
Vol. 50, No. 9, November, 1971
Printed in U.S.A.

Analysis and Design of Elementary Blinders for Large Horn Reflector Antennas

By DAVID T. THOMAS

(Manuscript received May 28, 1971)

An analysis of E-plane (transverse) radiation from horn reflector antennas for horizontal (transverse) polarization is presented. This analysis was based on Geometrical Theory of Diffraction with modifications to account for (i) finite *edges, (ii) grazing incident wave, and (iii) aperture illumination. Once proven valid for our purposes, the analysis was extended to permit blinders to be added to the antenna.*

Experimental and theoretical studies of single edge blinders have shown them to move the azimuth location of undesirable high sidelobes but not substantially reduce the sidelobe level. A half blinder, however, was shown to reduce the undesired 90-degree sidelobe to −62 dB, an 8-dB reduction. Simultaneously, sidelobe levels are below −62 dB for azimuths between 35 degrees and 180 degrees at both 3.74 and 6.325 GHz. Theoretical predictions indicate it is broadband at 4, 6, and 11 GHz. The half blinder also has excellent mechanical features.

I. INTRODUCTION

In recent years, demands have been made to improve the sidelobe performance of the Bell System horn reflector antenna. One demand is related to the Metropolitan Junction Concept* for radio relay route planning. This concept was initiated in the mid 1960's and resulted in narrower angles between radio relay routes converging on a junction point. Generally, increased service demands also added to route congestion and placed more stringent requirements on the antenna performance. A combined experimental and theoretical program was begun with the expressed purpose of reducing certain high sidelobes.

* In the Metropolitan Junction Concept, only radio relay routes terminating in a large city are brought into the city. All other routes bypass the city around a ring of stations about 20 miles out. This is contrary to the practice prior to the 1960's.

A previous paper[1] discussed improvements in the transverse-plane radiation levels for vertical (longitudinal) polarization (VP). This present paper is addressed to transverse-plane radiation for horizontal (transverse) polarization (HP).*

The horn reflector antenna[2] is a combination of a square electromagnetic horn and a reflector which is a sector of a paraboloid of revolution. A side view and front plane view of the antenna are illustrated in Fig. 1. The results given in this paper refer to the Bell System horn reflector antenna which has the following aperture dimensions:

Flare half angle	$\alpha = 14.5$ degrees
Front tilt angle	$\beta = 14.5$ degrees
Aperture side edge length	2.59 meters
Average aperture width	2.59 meters.

The intended frequency bands of operation are 3.70–4.20 GHz, 5.925–6.325 GHz, and 10.7–11.7 GHz.

One very interesting aspect of this antenna is the low inherent sidelobes in the azimuth (transverse) plane. For horizontal polarization, the sidelobe levels beyond 30 degrees are 60 dB or more below the main beam for the Bell System antenna, except for a major high-sidelobe region near 90 degrees with levels of about −52 dB at 3.74 GHz and −58 dB at 6.325 GHz.

The elimination of this high sidelobe region was the major purpose of this work. One approach earlier tried by R. R. Grady[1] was to add "blinders," i.e., change the shape of the side edges of the aperture. Although the blinder shapes tried by Grady moved the location of the major high-sidelobe region of the antenna, the overall reduction in sidelobe levels was insufficient for our purposes.

In order to expedite development of the complex blinder shapes which we felt would be necessary, a theoretical model was first developed for the original antenna and is presented here. This same model has been extended to predict the radiation patterns of horn reflector antennas with multiple edge shaped blinders attached.

II. GEOMETRICAL THEORY OF DIFFRACTION

The analytical method used for predicting the E-plane radiation was based on Geometrical Theory of Diffraction (GTD).[3,4] GTD has a long history of providing solutions to electromagnetics problems.

* Longitudinal polarization and longitudinal plane are aligned with the pyramidal horn axis. Transverse polarization and transverse plane are perpendicular to the horn axis.

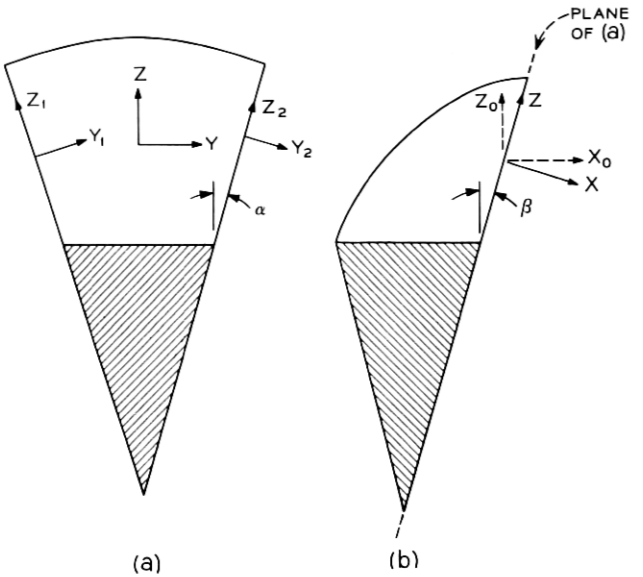

Fig. 1—Front and side views of a horn reflector antenna.

In situations similar to ours, GTD has successfully predicted the far sidelobe levels of pyramidal horn antennas[5–7] and other structures such as parallel plate waveguides.[8,9] In order to apply GTD to the problem at hand, it was necessary to account for (*i*) the *finite* length of each edge[10] and (*ii*) the incident wave direction *parallel* to the side walls of the antenna.[11] In addition, the illumination function with the TE_{10} incident mode in the horn was included. Also, as the azimuth angle passes 90 degrees, visually one edge disappears. To account for this phenomenon, the contribution of the disappearing edge was neglected when the azimuth angle exceeds 90 degrees, i.e., only singly diffracted rays were included. Two checks on the accuracy of our model were used: (*i*) the *measured* E-plane radiation pattern for HP at 3740 MHz, and (*ii*) radiation patterns computed by an approximate Kirchhoff *Aperture* Integral as described in a later section.

The incident wave in the pyramidal horn section is the TE_{10} mode with orientation depending on polarization. For horizontal polarization, the amplitude variation is sinusoidal from front to back and uniform from side to side. After reflection by the paraboloidal surface, the incident wave amplitude is tapered by the $1/R$ spherical attenuation and slightly distorted but, to a good approximation, the vertical

(longitudinal) variation is sinusoidal in the aperture. The diffracted fields of the top and bottom edges are neglected because of the near zero illumination there. The E-plane radiation will be determined solely by edge diffraction from the side edges of the aperture. At both sides, the E-field is perpendicular and the H-field parallel due to boundary conditions. The incident H-field near edge #1, to a good approximation, varies as

$$H^i_{z1} = H_o\, e^{jKX_a} \cos\left(\frac{\pi Z_1}{2b}\right) \cos\beta. \tag{1}$$

The coordinates used are shown in Fig. 1. The Appendix develops the equations necessary to relate the various coordinate systems.

The canonical problem of interest to us is edge diffraction by a semi-infinite plane which was first worked by A. Sommerfeld[12] in 1896. This canonical problem can be solved exactly, but we used the high-frequency asymptotic solution which describes the diffracted ray as

$$u_d = H_z = H^i_z\, D\, \frac{e^{+iKr}}{\sqrt{r}} \tag{2}$$

where r is the cylindrical radius from the edge, H^i is the incident wave, and D is the diffraction coefficient given by J. B. Keller[3] as

$$D = -\frac{e^{j\pi/4}}{\sqrt{8\pi K}\cos\beta}\left[\mathrm{CSC}\left(\frac{\phi' + \gamma}{2}\right) \mp \mathrm{CSC}\left(\frac{\phi' - \gamma}{2}\right)\right]. \tag{3}$$

The angles ϕ' and γ are shown in Fig. 2. Cos β is included to account

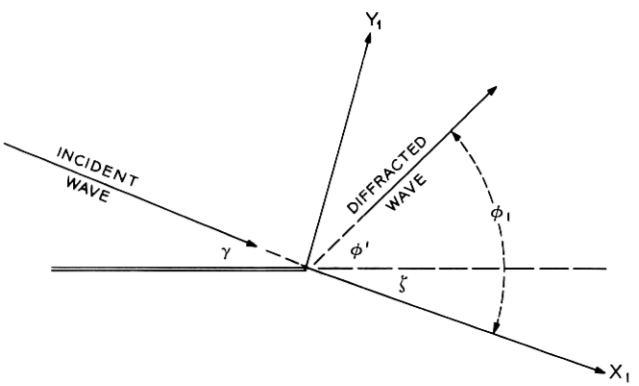

Fig. 2—Diffraction of a plane wave by a semi-infinite edge.

for the tilted aperture and the fact that the incident wave direction is not perpendicular to the aperture.

For a grazing incident wave (direction of propagation parallel to the sides) such as we have, γ is zero and only the first term of the diffraction coefficient remains,[11]

$$D = -\frac{e^{j\pi/4}}{\sqrt{8\pi K}\cos\beta}\,\mathrm{CSC}\left(\frac{\phi'}{2}\right). \tag{4}$$

The angle, ζ, which relates ϕ' and ϕ_1 as

$$\phi' = \phi_1 - \zeta \tag{5}$$

was found from the coordinate transformations in the Appendix to be defined by

$$\tan\zeta = \sin\alpha\tan\beta. \tag{6}$$

For the second edge, we found that

$$\phi' = \phi_2 + \zeta, \tag{7}$$

with ζ as given above.

The *finite* length of the diffracting edges has been considered by C. E. Ryan.[10] The diffracted field sources can be viewed mathematically as magnetic line currents. Since GTD is a *local* phenomenon, the use of magnetic currents is valid for finite edges as well. Taking into consideration the radiation patterns of finite length line currents, the *far zone* diffracted fields of the side edges become

$$H_{\theta 1} = -\frac{j\omega\epsilon}{4}\frac{2H_o b}{K}\frac{e^{+jKR_1}}{R_1}\,\mathrm{CSC}\,\frac{\phi_1-\zeta}{2}\sin\theta_1 \cdot \frac{\cos\left[Kb(\cos\theta_1 - \sin\beta\cos\alpha)\right]}{\frac{\pi^2}{4} - (Kb)^2(\cos\theta_1 - \sin\beta\cos\alpha)^2}, \tag{8}$$

$$H_{\theta 2} = +\frac{j\omega\epsilon}{4}\frac{2H_o b}{K}\frac{e^{+jKR_2}}{R_2}\,CSC\,\frac{\phi_2+\zeta}{2}\sin\theta_2 \cdot \frac{\cos\left[Kb(\cos\theta_2 - \sin\beta\cos\alpha)\right]}{\frac{\pi^2}{4} - (Kb)^2(\cos\theta_2 - \sin\beta\cos\alpha)^2}. \tag{9}$$

There remains only the superposition of $H_{\theta 1}$ and $H_{\theta 2}$ and the cal-

culation of radiation patterns. In the azimuth plane, ϕ_o will vary from 0 degrees to 180 degrees and θ_o is 90 degrees. Only the horizontal polarized field component, E_{ϕ_o}, contributes to the azimuth radiation pattern. Since H_{θ_o} corresponds to E_{ϕ_o}, the HP fields are

$$\bar{H}_{\text{HP}} = (\hat{\theta}_o \cdot \hat{\theta}_1) H_{\theta 1} + (\hat{\theta}_o \cdot \hat{\theta}_2) H_{\theta 2} . \tag{10}$$

The normalized *directivity* will be

$$G(\phi_o) = \frac{| \bar{H}_{\text{HP}} |^2_{\substack{\theta_o = \pi/2 \\ \phi_o}}}{| \bar{H}_{\text{HP}} |^2_{\substack{\theta_o = \pi/2 \\ \phi_o = 0}}} . \tag{11}$$

For azimuth angles 0 degrees to 90 degrees, equation (10) was used. Beyond 90 degrees, however, only one edge was assumed to be visible and the second edge contribution was neglected. The discontinuity at 90 degrees produced by this move is very small and the slightly improved accuracy which would result if doubly diffracted rays were used was not felt worth the additional work.

III. KIRCHHOFF APERTURE THEORY

In order to provide an independent check on the accuracy of our previous model, the radiation pattern was computed using Kirchhoff Aperture Integrals.[13,14] Once the incident fields, $\bar{E}^i(Y, Z)$, are known in the actual antenna aperture, the *far zone* radiated fields, $\bar{E}^s(R, \theta, \phi)$, are given by

$$\bar{E}^s = \frac{jK}{4\pi R} [e^{jKR}[\mathbf{R} \times (\mathbf{n} \times \bar{N}) - \mathbf{R} \times (\mathbf{R} \times (\mathbf{n} \times (\mathbf{n}_i \times \bar{N})))]] \tag{12}$$

where

$\mathbf{R}$ is the radial unit vector,

$\mathbf{n}$ is the outward unit normal to the aperture,

$\mathbf{n}_i$ is the unit vector in the direction of propagation of the incident wave,

and $\bar{N}$ is given by

$$\bar{N} = \iint_{\text{Aperture}} \bar{E}^i(Y, Z) e^{-jK(Y \sin\theta \sin\phi + Z \cos\theta)} \, dy \, dz, \tag{13}$$

and the integral is over the actual aperture—not the projected aperture. The coordinates XYZ are as shown in Fig. 1, with $R\theta\phi$ being the spherical coordinates associated with XYZ. For HP, N_Z is neglected and N_Y is found to be

$$N_Y = \frac{\pi ab}{-jKa \sin\theta \sin\phi} \cdot \left\{ e^{-jKa \sin\theta \sin\phi} \frac{\cos\left[Kb(\cos\theta - \sin\beta + \tan\alpha \sin\theta \sin\phi)\right]}{\frac{\pi^2}{4} - (Kb)^2(\cos\theta - \sin\beta + \tan\alpha \sin\theta \sin\phi)^2} - e^{+jKa \sin\theta \sin\phi} \frac{\cos\left[Kb(\cos\theta - \sin\beta - \tan\alpha \sin\theta \sin\phi)\right]}{\frac{\pi^2}{4} - (Kb)^2(\cos\theta - \sin\beta - \tan\alpha \sin\theta \sin\phi)^2} \right\}. \quad (14)$$

Coordinate transformations between θ, ϕ and θ_o , ϕ_o are given in the Appendix.

A computer program based on equations (8) to (11) was written to

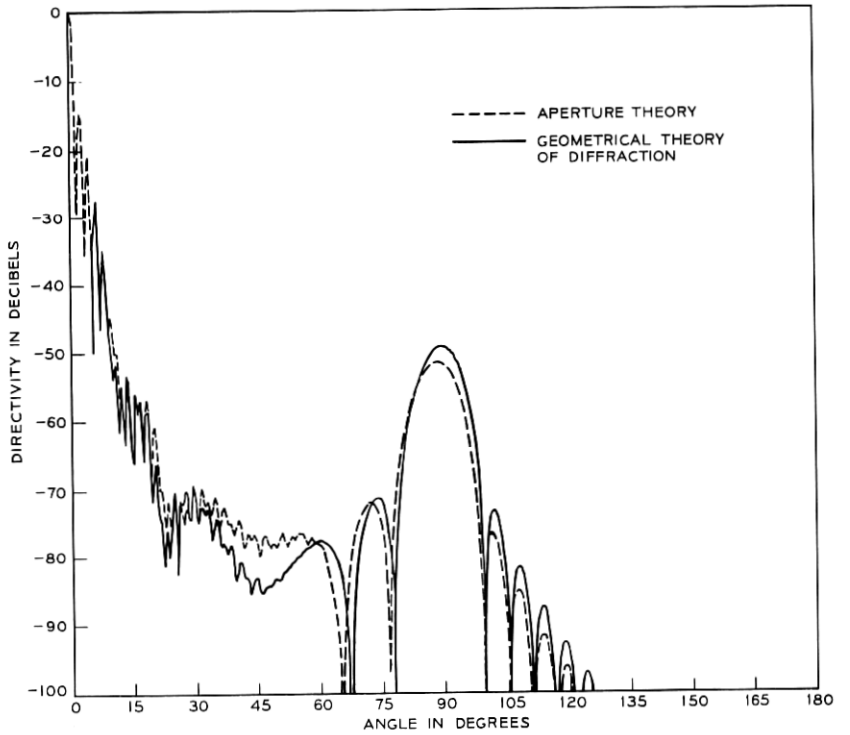

Fig. 3—Comparison of predicted transverse-plane (ϕ_o) radiation patterns of a horn reflector antenna using GTD and aperture theory (transverse polarization at 3740 MHz).

calculate and plot the *far zone* radiation pattern of the Bell System horn reflector antenna in the azimuth plane for horizontal polarization. Figure 3 compares the results with a similar radiation calculation using the approximate Kirchhoff Aperture Integral of equations (12) to (14). The agreement is remarkably good, which is somewhat surprising in view of the limitations of aperture theory. In this case at least aperture theory appears to be accurate for azimuth angles, ϕ_o , up to almost 90 degrees.

The necessity of using GTD instead of Aperture Integrals is twofold: (*i*) we are interested in far sidelobes beyond 90 degrees where Aperture Integrals are inappropriate, and (*ii*) the ultimate goal is a treatment of the antenna edges, multiple edge blinders, for example, which would require a degree of sophistication beyond the capacity of Aperture

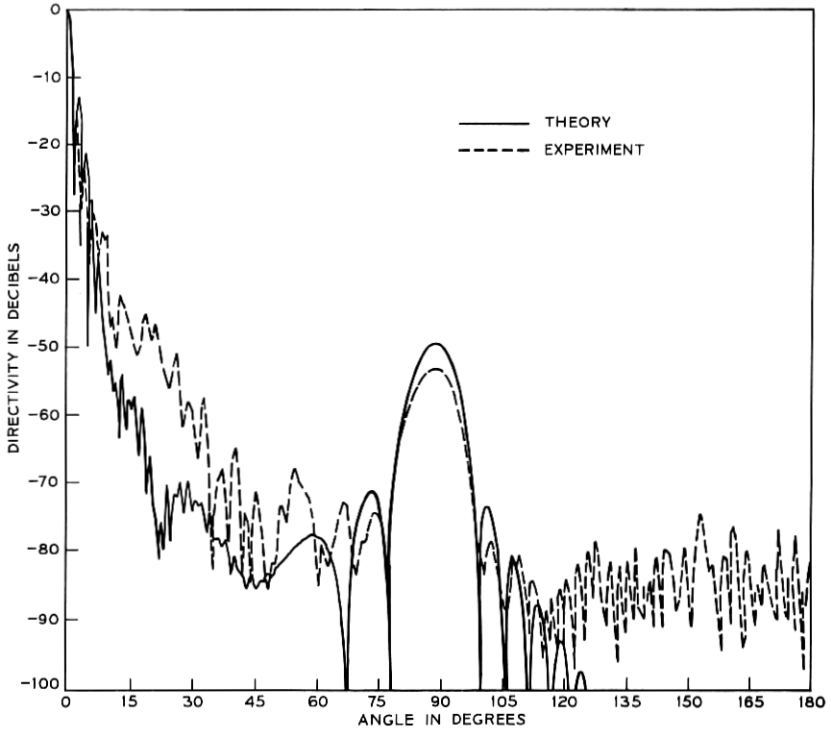

Fig. 4—Comparison of transverse-plane (ϕ_o) measured radiation and radiation predicted by GTD for the horn reflector antenna (transverse polarization at 3740 MHz).

Integrals but well within the capability of the GTD methods described here.

A comparison of GTD with a measured pattern appears in Fig. 4. The measured pattern was taken on a production model of the Bell System horn reflector antenna for HP and 3740 MHz. In the measurement it was necessary to tilt the antenna forward by 0.9 degree to aim it at the transmitting antenna. Taking this into account altered the theoretical GTD pattern of Fig. 4. The similarity of measured and theoretical patterns confirms the validity of the model. The early sidelobes ($\phi_o < 8$ degrees) agree precisely and our main concern, the high sidelobe near 90 degrees, is nicely predicted. Differences in sidelobe levels between GTD theoretical curves and experimental radiation patterns can probably be ascribed to inaccurate aperture illumination and minor structural differences between our model and the actual

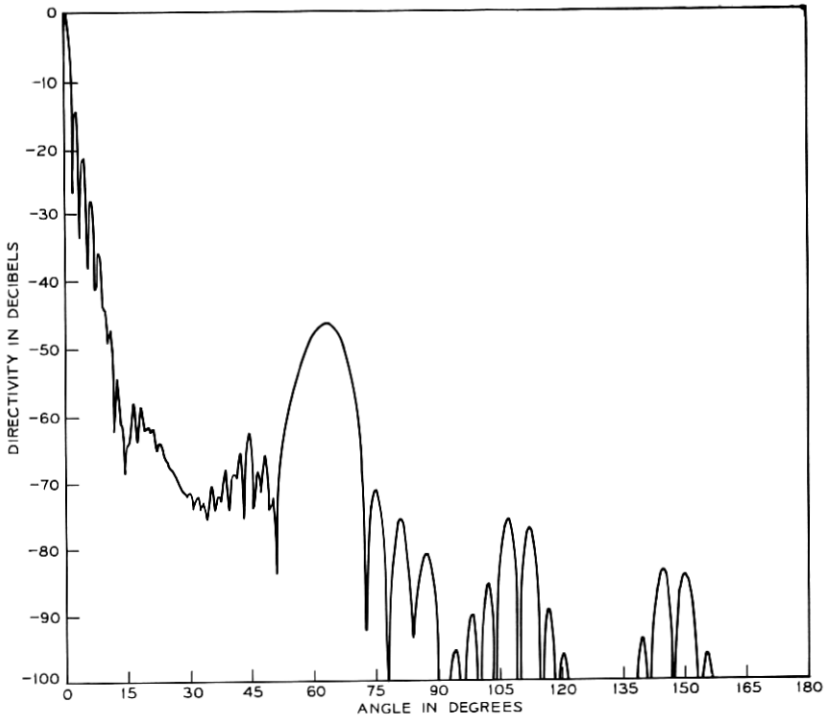

Fig. 5—Theoretical transverse (azimuth) plane radiation for horn reflector antenna with single edge blinder attached ($\beta = 25$ degrees)—transverse polarization (HP) at 3.74 GHz.

antenna. However, as a blinder design aid, the GTD model is entirely adequate.

IV. SINGLE EDGE BLINDERS

Grady[1] has reported measurements of the azimuth pattern for HP of the horn reflector antenna with single edge blinders attached. These single edge blinders alter the front tilt angle, β, and move the azimuth location of the high sidelobe but do little to reduce it. The theory described above was tested for single edge blinders and concurred with Grady, as illustrated in Figs. 5 and 6 for front tilt angles of 5 degrees and 25 degrees. Notice the major high sidelobe is moved but the level is only slightly changed.

A third single edge blinder tested analytically had a front tilt angle,

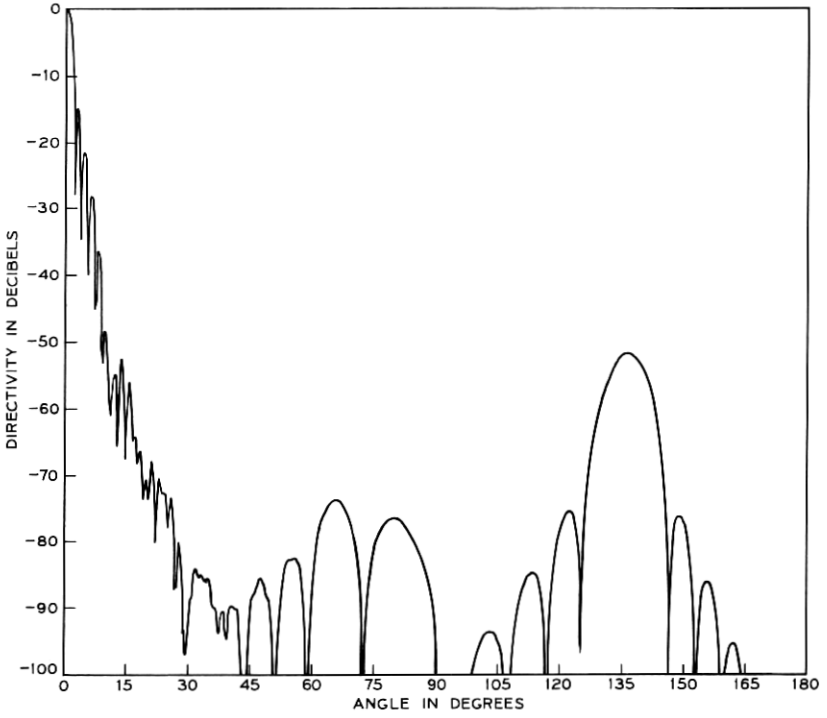

Fig. 6—Theoretical transverse (azimuth) plane radiation for horn reflector antenna with single edge blinder attached (β = 5 degrees)—transverse polarization (HP) at 3.74 GHz.

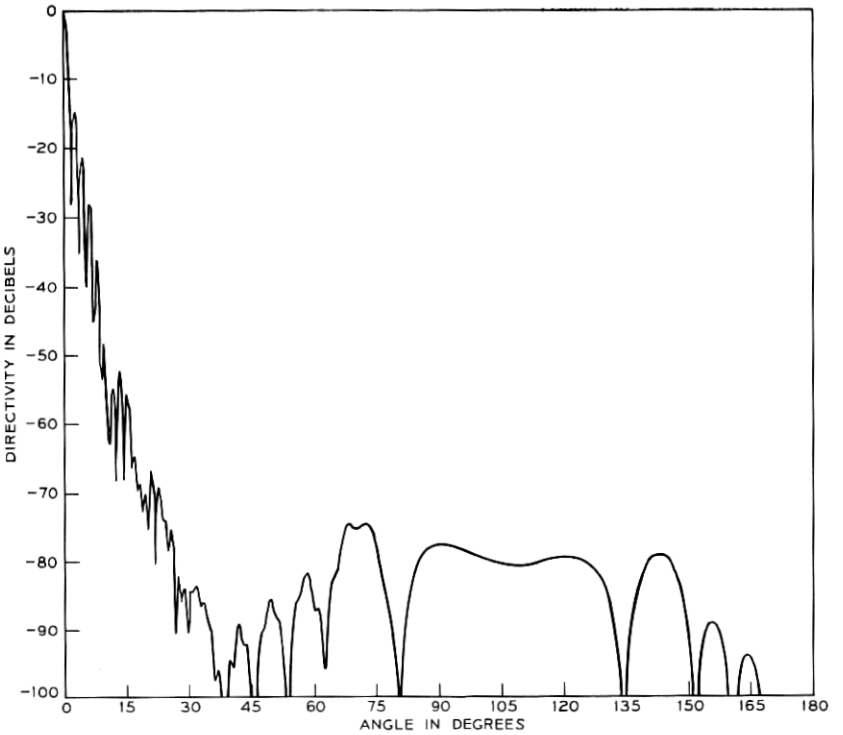

Fig. 7—Theoretical transverse (azimuth) plane radiation for horn reflector antenna with single edge blinder attached ($\beta = -5$ degrees)—transverse polarization (HP) at 3.74 GHz.

β, of -5 degrees. Whenever β is negative ($\beta < 0$ degrees), the major high sidelobe disappears completely in the azimuth plane, as is evident in Fig. 7. Apparently this blinder solves our problem but the large size of such a blinder creates difficult mechanical problems such as weight and windload. Making this blinder out of fine mesh wire might be an agreeable compromise but has not yet been tested.

A parametric study followed, leading to an equation which relates front tilt angle, β, to major sidelobe location, ϕ_H (in the azimuth plane), as

$$\phi_H = 2 \tan^{-1} \left(\frac{\tan \alpha}{\sin \beta} \right). \tag{15}$$

As seen earlier, when $\beta < 0$, the major sidelobe disappears.

So it would appear that a single edge blinder is not a satisfactory

fix for reducing the unwanted high sidelobe. The best one can do without huge blinders is move the sidelobe to an unobtrusive location, a poor solution since special engineering would be required for each site and at some sites no amount of special engineering would produce good results.

V. A HALF BLINDER FOR SIDELOBE REDUCTION

Since a single edge blinder did not achieve the desired sidelobe reduction, two edge blinders were tried. We observed in the theoretical analysis [equation (8)] that the far zone field, $\bar{H}$, is proportional to edge length. Since each front tilt angle, β, produces a strong high sidelobe at a specific angle, a division of the blinder length into two edges at different front tilt angles β_1 , β_2 would reduce the fields by half in the direction of each major sidelobe. Meanwhile, back at the main beam ($\theta = 0$ degrees), the energy transmitted would *not* be altered, since blinder shape does not affect the main beam. As a result, a *two-edge blinder* should produce two high sidelobes, each 6 dB lower than the high sidelobe of a comparable single edge blinder.

The actual two-edge blinder tested was a half blinder, which retained the original front tilt angle ($\beta_1 = 14.5$ degrees) for half the front edge. The other angle, β_2 , was taken to be 4.5 degrees in order to widely separate the high sidelobes of the two edges. This half blinder con-

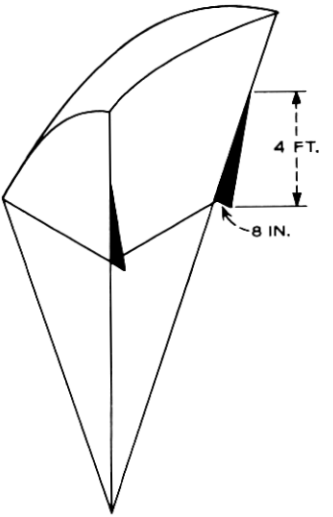

Fig. 8—Horn reflector antenna with half blinder attached.

figuration is shown in Fig. 8. Figure 9 compares the theoretical results for a horn reflector antenna with and without the half blinders attached. Notice the 6-dB reduction in sidelobe level of the 90-degree sidelobe, exactly as suggested above.

Based on the predicted sidelobe levels of the half blinder, a model was built for experimental tests. The dimensions of the half blinder built for testing were base 8 inches, height 4 feet, which provide an acute angle of about 10 degrees. A measured antenna pattern for HP at 3740 MHz is shown in Fig. 10 and compared with the theoretical curves for the same blinder. The comparison is quite good, with the two major sidelobe locations agreeing very well and the measured sidelobe levels 2 to 3 dB below predicted values. The 2- to 3-dB lower measured sidelobes occur quite consistently in all available comparisons of measured and predicted curves and are thought to be due to an

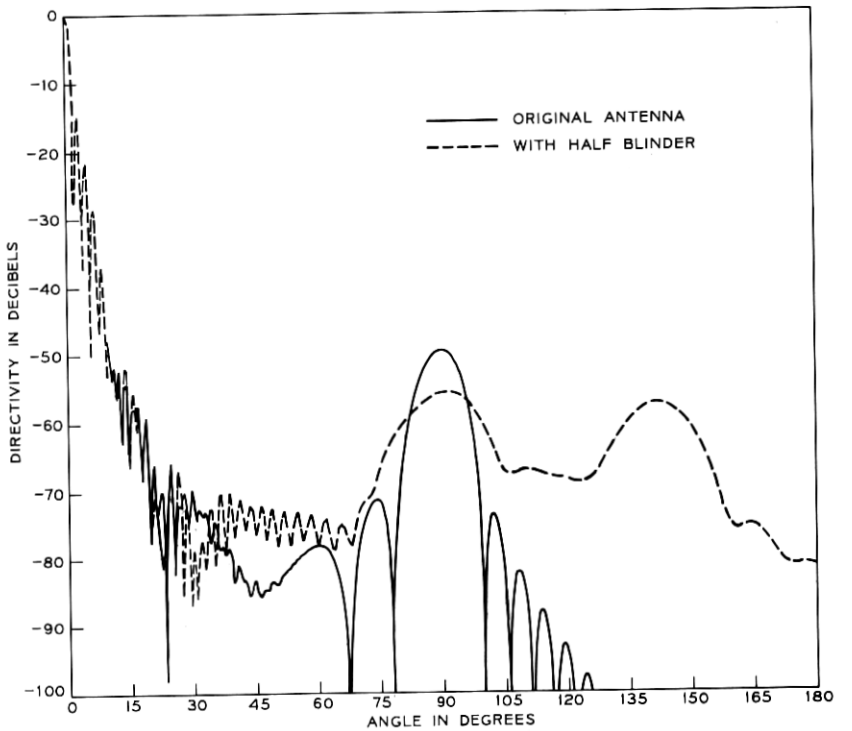

Fig. 9—Theoretical transverse (azimuth) plane radiation patterns for horn reflector antenna with and without half blinders attached—transverse polarization (HP) at 3.74 GHz.

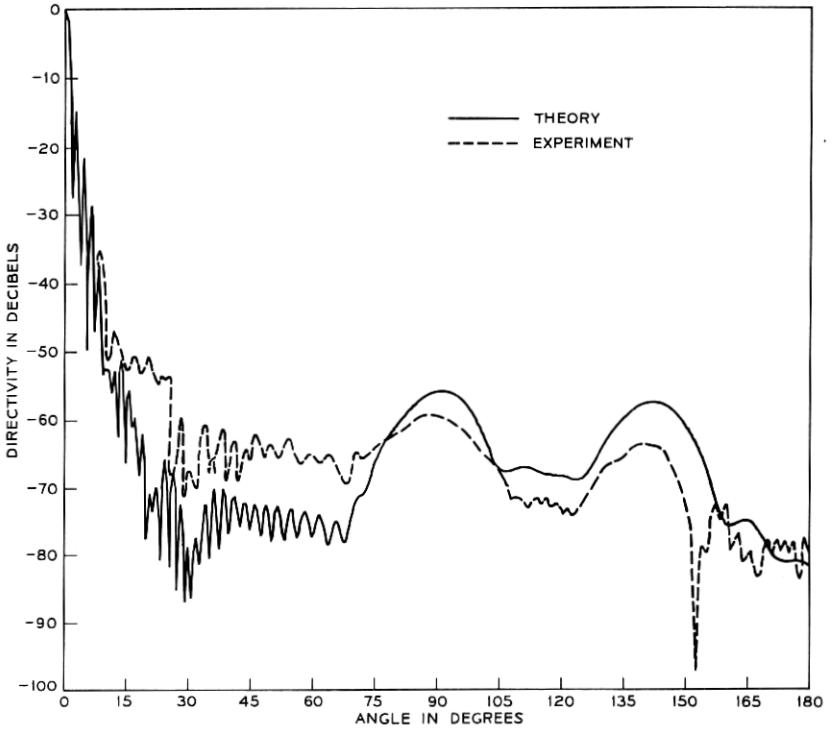

Fig. 10—Comparison of measured and GTD predicted transverse (azimuth) plane radiation of horn reflector antenna with half blinders attached—transverse polarization (HP) at 3.74 GHz.

unexpected amplitude taper near the edges of the antenna which was not used in the analytical model.

The sinusoidal distribution of incident energy in the aperture makes the fields strongest near the center (vertically) of the aperture. Hence, moving the half blinders up from the bottom should further reduce the high sidelobe near 90 degrees (now −59 dB). This is because more of the power diffracted by the edges would be diverted to the second high sidelobe near 140 degrees (which was somewhat lower). Experimentally adjusting for optimum sidelobes, it was found that 9 inches up from the bottom was best. For the half blinders located 9 inches above the bottom of the aperture, the measured pattern (3740 MHz, HP) is shown in Fig. 11. This final adjustment gave sidelobe levels −62 dB or below for azimuth angles from 35 degrees to 180 degrees, reducing the unwanted sidelobe to acceptable levels.

To verify the suitability of the half blinder for broadband operation,

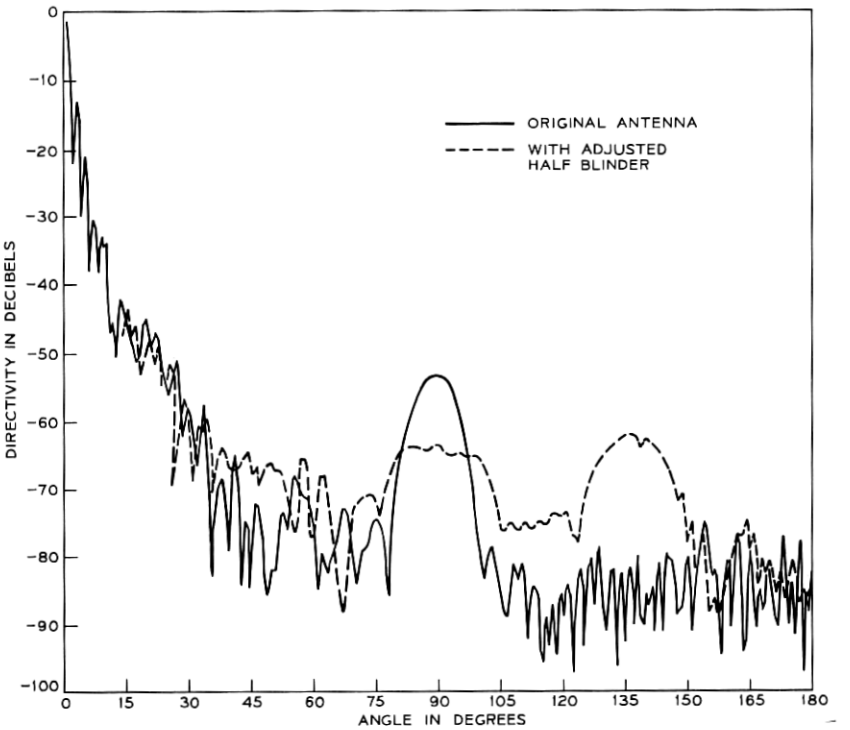

Fig. 11—Comparison of measured transverse (azimuth) plane radiation of horn reflector antenna with and without adjusted (up 9 inches) half blinders attached—transverse polarization (HP) at 3.74 GHz.

theoretical patterns were run for three frequencies (*high, middle, low*) in each of the 4, 6, and 11 GHz bands. These curves show that similar results are obtained in all three frequency bands and indicate better results should be obtained at 6 and 11 GHz. Of course, this is expected since 6 and 11 GHz patterns for the original antenna have lower sidelobes than for 4 GHz. Thus, we can expect good broadband performance of the half blinder in the three frequency bands.

Mechanically, the half blinder is ideal. Its small size (8 inches by 4 feet) makes it easy to fabricate and attach to existing antennas and the additional windload with it attached will be negligible.

VI. CONCLUSIONS

This paper reports results of research still in progress aimed at reducing undesirable high sidelobe levels in the E-plane radiation for

HP. Tests (both experimental and theoretical) of single edge blinders have shown that altering the front tilt angle, β, of the horn reflector succeeds in moving the location of the undesirable sidelobe but does not substantially reduce the level.

A half blinder attached to the antenna, however, reduced the undesirable 90-degree sidelobe level to 62 dB below the main beam, an 8-dB reduction. Simultaneously, radiation levels were maintained at or below -62 dB for all azimuth angles from 35 degrees to 180 degrees. The antenna response with half blinder attached has been theoretically predicted to be broadband at 4, 6, and 11 GHz and the mechanical features are excellent. Unfortunately, the raised radiation levels from 100 degrees to 150 degrees (through below -62 dB) and the unacceptable levels near 30 degrees indicate the half blinder may not be suitable for general application. Future writings will describe the design of many edged blinders and the effect of curved blinders on radiation levels.

VII. ACKNOWLEDGMENTS

The measured patterns were taken by Jack E. Millwater of the Antenna Design Department, Bell Telephone Laboratories, Whippany, New Jersey. Suggestions regarding the interpretation of the angles γ and ζ were made by T. S. Chu.

APPENDIX

It was helpful to describe the various coordinate systems to be used for the aperture and the edges. We needed various coordinate transformations in order to orient the edges correctly for the Geometrical Theory of Diffraction. Each side edge had its own coordinate, with origin at the center of the edge, and Z-axis directed along the edge. These are shown in Fig. 1. The appropriate coordinate transformations are:

$$\left.\begin{aligned} X_1 &= X \\ Y_1 &= (Y + a)\cos\alpha + Z\sin\alpha \\ Z_1 &= -(Y + a)\sin\alpha + Z\cos\alpha \\ X_2 &= X \\ Y_2 &= (Y - a)\cos\alpha - Z\sin\alpha \\ Z_2 &= (Y - a)\sin\alpha + Z\cos\alpha \end{aligned}\right\} \tag{16}$$

and, in addition,

$$\left.\begin{aligned} X &= X_o \cos\beta - Z_o \sin\beta \\ Y &= Y_o \\ Z &= X_o \sin\beta + Z_o \cos\beta \end{aligned}\right\} \tag{17}$$

where α, β, a, and b are described in Section I. In addition, spherical coordinates will be employed so we have a need for transformation of R, θ, ϕ into R_1 , θ_1 , ϕ_1 and R_2 , θ_2 , ϕ_2 . However, they are obtainable from the above equations and are not given except for radii R_1 , R_2 in the *far field*. They are

$$\begin{aligned} R_1 \text{ , } R_2 &= \sqrt{R^2 + a^2 \pm 2Ra \sin\theta \sin\phi} \\ R_1 \text{ , } R_2 &\approx R \pm a \sin\theta \sin\phi. \end{aligned} \tag{18}$$

These are needed for correct phase reference in superposing the two edge contributions.

REFERENCES

1. Grady, R. R., "Sidelobe Control in the Cornucopia or Horn Reflector Antenna," presented to National Electronics Conference, Chicago, Illinois, December 7–9, 1970.
2. Crawford, A. B., Hogg, D. C., and Hunt, L. E., "A Horn Reflector Antenna for Space Communication," B.S.T.J., *40*, No. 4 (July 1961), pp. 1095–1116.
3. Keller, J. B., "Geometrical Theory of Diffraction," J. Opt. Soc., *52*, (1962), pp. 116 ff..
4. Kouyoumjian, R. G., "Asymptotic High Frequency Methods," IEEE Proc., *53*, (1965), pp. 864 ff..
5. Rudduck, R. C., and Tsai, L. L., "Application of Wedge Diffraction and Wave Interaction Methods to Antenna Theory," from Application of Optical Methods to Microwave Problems, Ohio State University Short Course, 1969. [See also IEEE Trans., *AP-16*, (1968) pp. 83 ff..]
6. Russo, P. M., Rudduck, R. C., and Peters, L., Jr., "A Method for Computing E-Plane Patterns of Horn Antennas," IEEE Trans., *AP-13*, (1965), pp. 219 ff..
7. Yu, J. S., Rudduck, R. C., and Peters, L., Jr., "Comprehensive Analysis of Horn Antennas by Edge Diffraction Theory," IEEE Trans., *AP-14*, (1966), pp. 138 ff..
8. Ryan, C. E., and Rudduck, R. C., "A Wedge Diffraction Analysis of the Radiation Patterns of Parallel-Plate Waveguides," IEEE Trans., *AP-16*, (1968), pp. 490 ff..
9. Rudduck, R. C., and Wu, D. C. F., "Slope Diffraction Analysis of TEM Parallel-Plate Guide Patterns," IEEE Trans., *AP-17*, (November 1969).
10. Ryan, C. E., "Equivalent Current Concepts and Three Dimensional Radiation Solution," from Application of Optical Methods to Microwave Problems, Ohio State University Short Course, 1969.
11. Kouyoumjian, R. G., "An Introduction to Geometrical Optics and Geometrical Theory of Diffraction," from Application of Optical Methods to Microwave Problems, Ohio State University Short Course, 1969. (See also Ref. 3.)
12. Sommerfeld, A., *Optics*, New York: Academic Press, 1954, p. 261.
13. Stratton, J. A., *Electromagnetics*, New York: McGraw-Hill, 1941, p. 424.
14. Silver, S., *Microwave Antenna Theory and Design*, New York: McGraw-Hill, 1948, p. 162.